Table of content figure: Hit polymers discovered using high throughput combinatorial microarrays, exhibiting reduced bacterial attachment compared with commercial catheter materials.

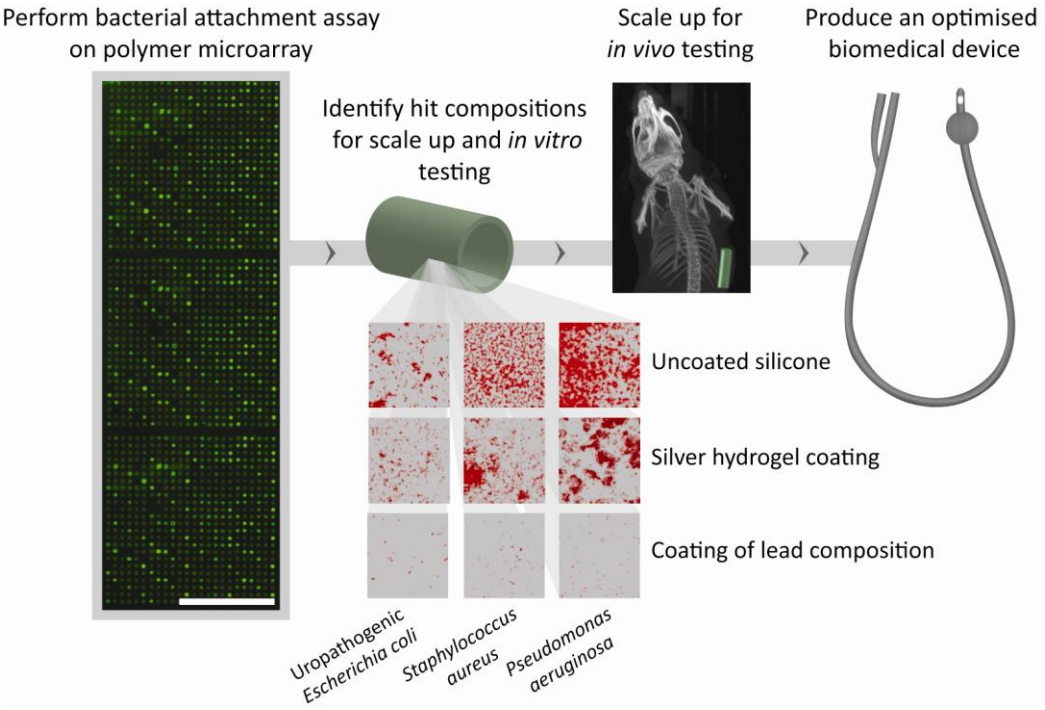

Combinatorial discovery of novel polymers resistant to bacterial attachment

Andrew L. Hook[1*], Chien-Yi Chang[2*], Jing Yang[1*], Jeni Luckett[2], Alan Cockayne[2], Steve Atkinson[2], Ying Mei[3], Roger Bayston[4], Derek J. Irvine[5], Robert Langer[3,6,7], Daniel G. Anderson[3,6,7], Paul Williams[2‡], Martyn C. Davies[1‡], Morgan R. Alexander[1‡]

Bacterial attachment and subsequent biofilm formation are key challenges to the performance of medical devices. In this study, a high throughput materials discovery approach is developed which utilises surface structure-property relationships generated by assessing the interaction of bacteria with hundreds of polymeric materials simultaneously in a microarray format. Using this system, a new group of structurally related materials comprising ester and cyclic hydrophobic moieties are identified that dramatically reduce the attachment of pathogenic bacteria (*Pseudomonas aeruginosa, Staphylococcus aureus* and *Escherichia coli*). Hit materials coated on silicone achieved up to a 30 fold (96.7%) reduction in bacterial coverage compared with a commercial silver hydrogel coating *in vitro* and were effective at resisting bacterial attachment *in vivo* in a mouse implant infection model. These novel polymers represent a new class of materials resistant to bacterial attachment that could not have been predicted from the current understanding of bacteria-surface interactions.

[*] These authors contributed equally to this work. ‡Joint senior authors. [1]Laboratory of Biophysics and Surface Analysis, University of Nottingham, Nottingham, NG72RD, UK, [2]School of Molecular Medical Sciences, University of Nottingham, Nottingham, NG72RD, UK, [3]Department of Chemical Engineering, Massachusetts Institute of Technology, Cambridge, Massachusetts 02139, USA, [4] School of Clinical Sciences, Queen's Medical Centre, University of Nottingham, Nottingham, NG72QH, UK, [5] School of Chemistry, University of Nottingham, Nottingham, UK, [6]David H. Koch Institute for Integrative Cancer Research, Massachusetts Institute of Technology, Cambridge, Massachusetts 02142, USA, [7]Harvard-MIT Division of Health Science Technology, Massachusetts Institute of Technology, Cambridge, Massachusetts 02142, USA.

Healthcare-associated infection is widely acknowledged as the most frequent adverse event in health care. It has been estimated that 80% of the infections acquired in hospitals involve biofilms[1], surface associated bacterial communities within which bacteria show up to 1000 times higher resistance to antimicrobials and host defences when compared with their planktonic counterparts[2,3]. Biofilms on the surface of medical devices provide the massive bacterial inocula responsible for manifesting disease and can also serve as gene pools for antibiotic-resistance conferring plasmids[4,5]. Most strategies for reducing biofilm associated infections focus on the modification of existing materials used to manufacture in-dwelling medical devices by the incorporation of antibiotics[6,7] or other antimicrobials such as silver salts, nitrofurazone, chlorhexidine, polymerised quaternary ammonium surfactants, antibacterial peptides and anionic nanoporous hydrogels[8-15]. These approaches are directed towards the killing of bacterial cells attached to a material, whereas greater efficacy in preventing biofilm formation could be realised by the design of new materials with inherent resistance to bacterial attachment that would prevent biofilm formation[16]. Previous attempts to use a low-fouling strategy include poly(ethylene glycol) brushes[17] and. zwitterionic polymers[18,19]. A significant limitation to the development of a material resistant to bacterial attachment is the poor understanding of the bacterial response to surfaces required for *ab initio* materials design. To overcome this constraint, we have developed a high throughput approach to study bacterial attachment in hundreds of materials in a parallel assay format that utilises polymer microarrays[20,21]. The microarray approach has previously proven useful for identifying polymeric materials that support stem cell attachment and outgrowth.[22-25] Here, microarrays were adapted to the combinatorial development of novel materials resistant to bacterial attachment, as depicted schematically in Fig. 1.

A library of 22 acrylate monomers was selected from those available commercially to provide a wide chemical diversity including ethylene glycol chains of various length, fluoro-substituted alkanes, linear and cyclic aliphatic, aromatic and amine moieties. To generate a large combinatorial space, 16 monomers (Fig. 1a[*1-16*]) were mixed as the major component with another 6 monomers (Fig. 1a[A-F]) at ratios of 100:0 (6 repeats), 90:10, 85:15, 80:20, 75:25 and 70:30 to create 576 monomer solutions. The monomer solutions were printed in triplicate as 300 μm diameter spots with a height of approximately 20 μm onto a poly (hydroxyl ethylmethacrylate) (pHEMA) coated

microscope slide where they were photopolymerised by a free radical mechanism to form the first generation combinatorial polymer microarray (Fig. 1b).

Three pathogens *Pseudomonas aeruginosa*, *Staphylococcus aureus* and uropathogenic *Escherichia coli* (UPEC)[26] were transformed with plasmids expressing the green fluorescent protein (GFP) gene to facilitate a high throughput screen using a fluorescent intensity readout (Fig. 2a). These pathogens were chosen as they represent both Gram-positive (*S. aureus*) and Gram-negative (*P. aeruginosa* and UPEC) bacteria and are frequently the cause of medical device-associated infections[27]. The polymer microarrays were incubated with a suspension of planktonic bacteria for each of the pathogens separately for 3 days (72 h) revealing a wide range of bacterial attachment levels (Fig 2b-d). To simulate *in vivo* conditions such as those encountered in the urinary tract, a microarray was conditioned with artificial urine for 72 h before incubation with UPEC and, in another experiment, the RPMI-1640 media was replaced with artificial urine for the full 72 h incubation with UPEC (Fig 2e-f). Biomineralisation was observed on some polymers as opaque deposits after conditioning in artificial urine and after culture in artificial urine in the absence of buffering (Supplementary Fig. S1) which stimulated greater bacterial attachment in all cases. The time period of this assay provided a sufficiently stringent assay for the identification of a set of 'hit' materials that resisted bacterial attachment (Supplementary Fig. S2). The fluorescence signal ($\mathcal{F}$) (equation 1) was used to quantify the level of bacterial attachment for each bacterial strain. A linear correlation (R^2 = 0.93) between $\mathcal{F}$ and surface coverage measured by confocal measurements of polymer spots after incubation with UPEC confirmed the utility of $\mathcal{F}$ as a reliable estimate of bacterial coverage (Supplementary Fig. S3). In cases where polymers were formed from monomers that had opposing influences on bacterial attachment, a linear correlation between systematic variations in material composition and $\mathcal{F}$ was observed (Supplementary Fig. S4). For some polymer compositions the biological behaviour of the copolymer was superior to the homopolymers of the two monomer constituents. In one such example, shown in Supplementary Fig. S5, the $\mathcal{F}$ of *P. aeruginosa* ($\mathcal{F}_{PA}$) measured on the copolymer of monomer 11:C (80:20) of 0.26 ± 0.1 x 10^6 arbitrary units (AU) was lower than the homopolymer of 11 ($\mathcal{F}_{PA}$ = 0.52 x 10^6 ± 0.05 x 10^6 AU) and the copolymer of monomer 11:C (70:30) ($\mathcal{F}_{PA}$ = 0.42 x 10^6 ± 0.01 x 10^6 AU). This synergistic effect was observed for 11 of the 96

monomer pairs explored in the first generation array and in all cases led to improved resistance to bacterial attachment, demonstrating the importance of screening for hit materials within a copolymer library.

Varying levels of attachment were observed for the three bacterial species to different polymer surfaces (Supplementary Fig. S6). This finding is not surprising given the different surface properties and macromolecular surface composition of Gram-positive and Gram-negative bacteria[28] and the diverse attachment mechanisms employed which can involve surface proteins, flagella, fimbriae[29] and exopolysaccharides[30].

To assess the resistance of any given material to diverse bacterial species and strains and as a guide to selecting hit monomers for further study, a composite bacterial attachment parameter was developed. The $\mathcal{F}$ value from each strain on each polymer composition, including UPEC incubated on artificial urine conditioned slides and incubated in artificial urine, was normalised to the maximum GFP fluorescence intensity on the slide and averaged over all three replicates to produce a *bacterial performance value*, iota ($\imath$) (equation 2). The value of $\imath$ is plotted in an intensity map for all generation 1 polymers in Fig. 2g, revealing materials that have a high attachment of all three bacterial strains (shown as red) and those with a low attachment of all three (presented as blue). In order to compare the performance of each monomer used to fabricate the polymers, the average $\imath$ from each of the materials containing a given monomer was determined. These average *ί's* are shown in Fig. 2h ranking the monomers corresponding to their ability to prevent bacterial attachment, considering the major and minor monomers separately. Of all the monomers, monomers 8 and B produced materials with the lowest average $\imath$, whilst monomers 7 and E produced materials with the highest average $\imath$.

To investigate the influence of polymer surface properties on bacterial attachment, high throughput surface characterisation (HT-SC) of the polymer microarray was undertaken[31]. Techniques that probe the outermost surface of materials were employed; X-ray photoelectron spectroscopy (XPS) for quantitative elemental and functional analysis, atomic force microscopy (AFM) for topographical characterisation, time of flight secondary ion mass spectrometry (ToF-SIMS) for molecular characterisation, and water contact angle (WCA) measurement to probe the surface wettability[20,31-34]. The influence of each property on bacterial attachment was assessed for all three bacterial strains separately. No correlation was identified between bacterial attachment and surface

elemental composition (Supplementary Fig. S7), WCA or roughness (Supplementary Fig. S8), for the 496 materials studied on the first generation array. ToF-SIMS analysis coupled with the chemometrics technique of partial least square (PLS) regression has been demonstrated as a powerful technique for correlating surface chemistry represented in ToF-SIMS spectra with a univariate data set such as water contact angle[33] or stem cell attachment[24,25,35], and was applied here to search for correlations between the surface chemistry of the array with the $\mathcal{F}$ values from each strain and to identify important surface moieties for bacterial attachment.

The PLS regression model produced by this analysis successfully predicted the $\mathcal{F}$ values for *P. aeruginosa* and *S. aureus* from the ToF-SIMS spectra (Fig. 3a) as evidenced by the linear relationship between the predicted and experimental $\mathcal{F}$ values, shown in Fig. 3b-d, with an R^2 value of 0.68 and 0.76 for the two bacterial species, respectively. The PLS model for *S. aureus* gave a good prediction of the bacterial performance for all polymers except those containing monomer 1, 6 or 10. No correlation was identified for UPEC (R^2 = 0.28). Only 17% of the materials on the array had a $\mathcal{F}_{\text{UPEC}}$ value greater than 1% of $\mathcal{F}_{\text{UPEC }max}$ compared with 97% and 96% for *P. aeruginosa* and *S. aureus*, respectively. The low attachment of this strain on the materials screened made it difficult to compute a suitable PLS regression model; thus, this lack of a correlation does not exclude the possibility of a dependence of UPEC bacterial attachment on surface chemistry.

The successful prediction of bacterial attachment by *P. aeruginosa* and *S. aureus* from the ToF-SIMS spectra demonstrates that the attachment of these strains is dependent on the surface chemistry. More specifically, the influence of each of the hundreds of ions in the SIMS spectra on bacterial attachment is quantified by the regression coefficient (RC) where a positive coefficient indicates that the ion in question promotes whilst negative ones resist bacterial attachment (Fig. 3e). The surface chemical moieties assigned to fragments with the highest PLS RC are shown in Fig. 3e for both *P. aeruginosa* and *S. aureus*. In general, hydrocarbon secondary ions correlated with low bacterial attachment and oxygen containing ions from certain pendant groups were observed for high bacterial attachment for both *P. aeruginosa* and *S. aureus*. In particular, ions from cyclic carbon groups (C_4H^-, C_6H^-), ester groups (CHO_2^-), the tertiary butyl moiety ($C_4H_7^+$) and ions from aliphatic groups ($C_2H_3^+$, $C_2H_5^+$, $C_3H_7^+$) were correlated with lower bacterial attachment for both pathogens. Ions from ethylene glycol groups ($C_2H_3O^+$, $C_2H_3O_2^-$), and hydroxyl containing fragments ($C_4H_5O_2^-$, $C_6H_{11}O_3^-$) correlated with higher bacterial

attachment. These results point to the influence of moieties from particular monomers that are associated with the biological performance of the resultant polymer; bacterial attachment is reduced by the cyclic carbon environments in monomers 4 and B, the relatively higher density of ester groups in materials formed from the triacrylate monomers 13 and 15, the tertiary butyl group of monomer 5 and the dimethyl hydrocarbon segment on monomers 2, 8 and 12. Bacterial attachment is increased by the ethylene glycol group on monomer 1, 9, 16 and A and the hydroxyl group on monomers 6, 7, and 10.

To determine the best monomer composition to resist attachment by all three bacterial pathogens a second generation array was formulated that focussed on the hit constituents from the first generation array (Fig. 1d) but with greater variation in composition for each monomer pair. Monomer 4 was included as it contained the cyclic hydrocarbon moieties identified by the ToF SIMS ions, C_4H^- and C_6H^-, revealed to be associated with low bacterial adhesion by the PLS regression analysis. The top 4 hit monomers were selected (15, 5, 8 and B) and mixed with each other and monomer 4 at ratios of *x*:(1-*x*) where *x* varied from 10 to 90. This array contained 145 different materials (4 replicates of each) plus 4 materials selected as positive controls that exhibited high bacterial attachment from the first generation array. Attachment after 3 days of incubation with all three bacterial pathogens including UPEC incubated with artificial urine conditioned slides was assessed for the array and the *i* for each material determined (Fig. 4).

The top 6 copolymer compositions and 4 corresponding homopolymers with low bacterial attachment were chosen from the bacterial screen on the second generation array for scale-up from the microarray spots to 8-10 mm diameter sample *coupons* to investigate the scalability of the polymer's physico-chemical properties and biological performance (Supplementary Fig. S9-10). Initial scale up experiments included monomer 15 (and other triacrylates) but resulted in the formation of brittle materials that were observed to crack during the solvent extraction step. This was consistent with the formation of highly cross-linked polymer and, thus, monomer 15 was removed from subsequent scale up experiments. The bacterial coverage was found to be at least 2-fold lower on all scaled up materials compared with the positive control (Supplementary Fig. S9a). Confocal microscopy coupled with live/dead staining (Supplementary Fig. S10) on the scaled-up polymer coupons revealed that, in common with the control polymer, a mixture of live and dead attached bacteria are observed. To simulate the more challenging

in vivo conditioning by urine likely to occur on urinary catheters, *P. aeruginosa*, *S. aureus* and *UPEC* were incubated with polymer coupons pre-conditioned with artificial urine. For all three strains a greater than 3-fold reduction in bacterial coverage was observed for this assay compared with the positive control (Supplementary Fig. S9b), suggesting these materials are able to resist bacterial attachment in the presence of urine components. SIMS of the polymer coupons suggested that the aliphatic pendant group on monomers 4 and 8 was surface enriched compared with the equivalent microarray spots, which altered the respective materials' biological performance (Supplementary Fig. S9,11).

To prove the concept of these hits as potential medical device coatings monomers were dip coated and cured on silicone catheters (Fig. 1e) and bacterial attachment was compared to silicone catheters and a commercially available state-of-the-art silver containing coating. The 4 homopolymers of the hit monomers, 6 hit copolymer formulations and a positive control for each bacterial pathogen were coated along the luminal and abluminal surfaces of the catheters (Fig. 1f-g), ascertained by SEM (Supplementary Fig. S12). The coated catheters were then incubated with *P. aeruginosa*, *S. aureus* or UPEC for 72 h. Representative confocal images from the coated catheters after bacterial incubation are shown in Fig. 5a and the quantified biofilm coverage for each bacteria and corresponding *i* normalised to the biofilm coverage measured on silicone are shown in Fig. 5b.

In all cases the coated catheters had substantially lower bacterial coverage than the silicone elastomer for all three pathogens. A number of the 'hit' acrylate materials also exhibited a superior performance to the silver-hydrogel (BactiGuard®) coated latex catheter (Bardex®), which has been shown to be clinically effective at reducing catheter associated asymptomatic bacteriuria when compared with standard latex catheters[36]. It should be noted that the prevention of bacterial attachment to silver-hydrogel catheters is considered to be a consequence of the toxicity of silver ions to the bacteria, which is a different principle to the prevention of attachment by our 'hit' polymer coatings. The lowest surface coverage for *P. aeruginosa* was the homopolymer of monomer 4 that had a bacterial surface coverage of 1.2% ± 0.5% representing a 28 fold reduction compared to the silicone catheter and 17 fold lower than the BactiGuard® coated Bardex® catheter, for *S. aureus* was the copolymer of monomers B:5 (70:30) with a bacterial surface coverage of 0.5% ± 0.3% (67 fold reduction compared to silicone; 30 fold reduction compared to BactiGuard®), and for UPEC was the copolymer of B:4 (90:10) with a bacterial surface coverage of

1.2% ± 0.6% (9 fold reduction compared to silicone; 6 fold reduction compared to BactiGuard®). The homopolymer of B produced the catheter coating with the lowest *i* of 2.0% ± 1.0%, hence best preventing the attachment of all three different bacterial pathogens. The surface coverage on this coating was 2.3% ± 1.3%, 1.0% ± 0.4%, and 1.5% ± 0.7% for *P. aeruginosa*, *S. aureus* and UPEC, respectively. This amounted to a 12-fold reduction in the composite parameter ί compared with an uncoated silicone catheter and 7-fold lower than the silver embedded BactiGuard® coated Bardex® catheter.

There are a number of different strategies reported in the literature to reduce bacterial attachment to surfaces which are not yet commercially available; Zwitterionic coatings function by attachment prevention.[18,19] Comparison with the performance of our hits to these literature reports is difficult since experimental methodologies vary significantly. Attachment of *P. aeruginosa* (PA01) has been reported to be reduced by 25 fold compared to glass after 3 h incubation on a poly(sulfobetaine methacrylate) grafted surface[19] and in an incubation time closer to ours, a poly(carboxybetaine methacrylate) grafted surface reduced attachment of PA01 by 11 fold after 96 h bacterial exposure compared to glass[18].

The absence of a correlation between bacterial attachment and the contact angle or roughness of the materials studied (Supplementary Fig. S8) suggests that the interaction of bacteria with the methacrylate/acrylate library cannot be explained simply by hydrophobic interactions or roughness only, as previously invoked to explain bacterial performance on self-assembled monolayers, stainless steel and certain polymers[37]. It should be noted that the bacterial cell incubation experiments were not conducted under flow conditions, thus, this assay did not assess any advantage gained from the shielding from shear that increased roughness could provide. The ability to predict the bacterial attachment from the chemistry of the materials as represented by the ToF-SIMS spectra (Fig. 3(b-d)) confirms that the bacteria-material interaction is dependent on the surface chemistry. The PLS regression highlighted the ethylene glycol moieties employed in these libraries and hydroxyl groups for promoting the attachment of *P. aeruginosa* and *S. aureus.* The increased attachment associated with surface hydroxyl groups suggests a role for hydrogen bonding, which may be through an interaction with the lipopolysaccharides/lipoteichoic acids/exopolysaccharides present on the bacterial cell surface[30]. For reduced bacterial attachment, the PLS regression analysis identified hydrophobic moieties such as aromatic and aliphatic

carbon groups when accompanied by the weakly polar ester groups. By comparison with polystyrene, a purely hydrophobic material that is well known to support bacterial attachment (Supplementary Fig. S13)[38], the role of the ester group and the weakly amphiphilic structure of these hit polymers appears to be important for reduced bacterial attachment. Antibacterial behaviour has previously been reported on zwitterionic materials[19] where disparate chemical properties are presented in close proximity on the molecular scale analogous to the weak amphiphiles identified in our work. To further investigate the role of amphiphilic materials for preventing bacterial attachment, a third polymer microarray was produced that contained homopolymers of 15 methacrylate/acrylate monomers that had aliphatic, cyclic or aromatic pendant groups. $\mathcal{F}$ for *P. aeruginosa*, *S. aureus* and UPEC and ί for each material is shown in Supplementary Fig. S14. The relatively high bacterial attachment observed for *P. aeruginosa* provided the greatest distinction between the materials. The 6 materials with the lowest $\mathcal{F}_{PA}$ all contained cyclic or aromatic hydrocarbon groups. In contrast, the 6 materials with the highest ί all contained linear aliphatic carbon pendant groups, suggesting that the presence of ring structures are a determining factor for preventing bacterial attachment to methacrylate/acrylate polymers (Supplementary Fig. S14).

Confocal microscopy revealed neither dead nor living bacteria on the hit materials after 72 h incubation with planktonic bacteria (Fig. 5a) indicating that the mechanism behind the low attachment is adhesion prevention rather than a mechanism involving killing. Consistent with this conclusion, growth curves showed no inhibition by the 'hit' polymers for the bacterial strains used (Supplementary Fig. S15) and live/dead staining of UPEC biofilms revealed both live and dead cells present within the biofilm, which is typical of biofilms (Supplementary Fig. S10). Furthermore, there is no evidence of cytotoxicity relating to the polymers since the materials have elsewhere been shown to support the culture of delicate embryonic stem cell lines[24].

The ability of the lead acrylates discovered to resist the attachment of bacteria is likely to depend on the ability of bacterial cells to sense and respond to their immediate environment. This may be a consequence of the individual cells or the bacterial population collectively sensing the nature of the polymer surface via their cell envelope associated sensory proteins or via specific surface structures such as flagellar and pili involved in near-surface movement[39] or even through quorum sensing (bacterial cell-to-cell communication) mechanisms[40] such that the lack of bacterial attachment occurs through these decision making processes rather than simply being a

consequence of physico-chemical interactions between the bacteria and surface alone. Specific examples include the Rcs sensor kinase which controls the expression of a number of *E. coli* genes in response to growth on a solid surface[41] Furthermore, production of the *P. aeruginosa* exopolysaccharides Pel and Psl are both under quorum sensing control[42]. Thus, it is highly likely that bacterial responses to surfaces are more sophisticated than currently appreciated.

The *in vivo* environment is normally far more challenging than *in vitro* assessment for candidate medical materials. We therefore carried out a subcutaneous foreign body infection model to test the efficacy of one of the hit materials (Fig. 1h). A copolymer of monomer 4 and di(ethylene glycol) methyl ether methacrylate (DEGMA) amenable to the dip-coating methodology was prepared by catalytic chain transfer polymerisation (measured properties of the resultant polymer are shown in the Supplementary Table. S1). The DEGMA was included to tune the polymer's mechanical properties for *in vivo* use without compromising the polymer's resistance to bacterial attachment (Supplementary Figs. S16 and S17) and to exploit the ability of the oligo(ethylene glycol) moiety to reduce protein fouling[43] in the high protein containing environment.

Both control silicone and dip-coated silicone catheters were, implanted subcutaneously into mice and inoculated with bioluminescent *S. aureus* Xen29. Immediately following inoculation similar bioluminescence was observed for both coated and uncoated catheters (Fig 6). After 1 day, >10 fold reduction in bioluminescence was observed on the coated catheters compared with the uncoated silicone, a difference that persisted for 4 days (Fig. 6a-c). Bioluminescence requires the bacteria to be respiring aerobically, thus, will not detect bacteria that are viable but are either dormant or growing anerobically. To confirm reduced bacterial numbers, the mice were sacrificed on day 4 and the numbers of bacteria were quantified at the infection site (both the catheter and surrounding tissue), kidneys and spleen. Bacterial numbers were reduced by nearly two orders of magnitude on the coated catheter compared to the uncoated catheter, whilst an order of magnitude reduction in bacterial numbers was observed in the tissue surrounding the implant, the kidneys and the spleen, suggesting a reduced amount of systemic bacteria (Fig. 6e). The reduction in bioluminescence on the coated catheter in the live animal demonstrates that the coating successfully reduced bacterial survival compared to the silicone control. We interpret the persistence of bacteria on the silicone catheter as indicative of bacteria that were able to attach to the silicone and form resistant biofilms

thereby avoiding clearance by the host defenses. These observations clearly suggest that the performance of the 'hit' polymer identified *in vitro* translates to the challenging *in vivo* environment where reduced bacterial attachment and biofilm formation on the device is observed in the live animal and post mortem examination indicates reduced local and systemic infection. Sufficiently small diameter (2.7 mm) silver containing hydrogel coated catheters are not commercially available for the mouse model employed, preventing comparison of the *in vivo* performance with the *in vitro* experiments.

In summary, a high throughput methodology has been developed for the discovery of polymeric materials resistant to bacterial attachment using high throughput surface characterisation and chemometrics, which has identified novel simple chemical moieties that reduce bacterial adhesion to surfaces. The hit compositions discovered represent a new class of materials exhibiting resistance to bacterial attachment, which could not have been predicted from the current understanding of bacterial-material interactions. An *in vitro* comparison after 3 days incubation revealed up to a 67-fold reduction in bacterial coverage compared with a commercial uncoated medical grade silicone and a 30-fold lower bacterial coverage than a commercial silver hydrogel coating. The coating's resistance to bacterial attachment was demonstrated *in vivo* using a murine foreign body infection model confirming the potential of the hit materials as coatings for biomedical devices. By further developing this high throughput screening approach to include other bacterial species (including freshly isolated clinical strains), pathogens specific to particular niches and different growth conditions (representative of different environments), new polymeric materials may be found that are resistant to combinations of pathogens for specific medical devices, water purification systems, food preparation surfaces and utensils, or any scenario where bacterial adhesion is problematic. In contrast to killing mechanisms, the anti attachment mechanism does not place selective evolutionary pressure on organisms to develop antibiotic resistance.

Methods

Polymer array synthesis. Polymer microarrays were synthesised using methods previously described[22]. Monomers were purchased from Aldrich, Scientific Polymers and Polysciences and printed onto epoxy-coated slides

(Xenopore) dip-coated into 4% (w/v) pHEMA (Aldrich) using 946MP6B pins (ArrayIt) and a Pixsys 5500 robot (Cartesian) or a XYZ3200 dispensing workstation (Biodot). The arrays were dried at <50 mTorr for at least 7 days.

High throughput surface characterisation. Arrays were characterised by AFM, WCA, XPS and ToF-SIMS (see supplementary methods). The ToF-SIMS spectra data were analysed using principle component analysis (PCA)[44], and the correlation between ToF-SIMS spectra and bacterial adhesion was analysed using partial least squares (PLS) regression[35]. Both multivariate analysis methods were carried out using the Eigenvector PLS_Toolbox 3.5.

Scale up of materials. Selected compositions were scaled up to 10 mm polymer coupons. These were prepared by casting 5 µl of monomer solution (75% (v/v) monomer, 25% (v/v) DMF and 1% (w/v) 2,2-dimethoxy-2-phenyl acetophenone) onto epoxy-functionalised slides (Xenopore) dip-coated with 4% (w/v) pHEMA in ethanol. For growth inhibition studies, 40 µl of monomer solution was pipetted into a well of a 96 well microwell plate. Samples were irradiated with UV (365 nm) for 10 mins to initiate polymerisation with O_2 < 2000 ppm. The samples were dried at <50 mTorr for at least 7 days. To produce coated catheters, 4 cm long silicone lengths were cut from a silicone Foley urinary catheters (Bard, outer diameter 7.3 mm –*in vitro* or 2.7 mm -*in vivo*). The inside and outside surface was oxygen plasma treated for 5 min at 50 W. For *in vitro* use, plasma treated catheters were immediately immersed in monomer solution for 10 s and blotted to remove excessive monomer solution before photopolymerisation using UV (365 nm) for 1 min, with O_2 < 2000 ppm. For *in vivo* studies, plasma activated catheters were dip-coated with a 20% polymer solution in dichloromethane. The samples were then dried at <50 mTorr for at least 7 days. Polymer for *in vivo* studies was prepared by catalytic chain transfer polymerisation (see supplementary methods). The resultant polymer solution was used for coating silicone catheters without further purification. Uncoated silicone catheters and BactiGuard® (silver containing hydrogel) coated latex catheters (Bardex®) were used as controls. SEM imaging of coated catheters was conducted on a Jeol 6060LV variable pressure SEM. Samples were gold coated prior to imaging using a Leica EM SCD005 sputter coater.

Bacterial Growth Conditions. Three different bacterial species, *P. aeruginosa* PAO1, *S. aureus* 8325-4 and UPEC were routinely grown on either LB (Luria-Bertani, Oxoid, UK) agar plates at 37 ^{o}C or in broth at 37 ^{o}C with 200 rpm shaking. Three constitutively GFP expressing plasmids, pGFP[45], pSB2019 and pSB2020[46] were transformed into *P.*

aeruginosa PA01, *S. aureus* 8325-4 and UPEC respectively and maintained by adding appropriate antibiotics to the culture media. RPMI-1640 chemically defined medium (Sigma, UK) and artificial urine[47] were used in biofilm experiment for standardising the conditions and mimicking CAUTI, respectively. For the *in vivo* study *S. aureus* Xen29 (Caliper), were routinely grown on Tryptic soya Broth (Oxoid, UK) at 37 ^{o}C until an OD of 0.8, washed twice in phosphate buffered saline (PBS, Oxoid, UK) and stored in aliquots of $1x10^{9}$ cfu in PBS/20% glycerol. These were then thawed and diluted with PBS prior to injection into the lumen of the catheter.

Prior to incubation with the bacteria, the microarray slides were washed in distilled H_2O for 10 min, air-dried and UV sterilised. Artificial urine conditioned slides were incubated for 72 h at 37 ^{o}C in 15 ml of artificial urine with 5% CO_2. Subsequently, slides were washed 3 times in RPMI-1640 medium or artificial urine. Bacteria were grown on polymer slides under similar conditions to those previously described[48,49]. Briefly, UV-sterilised polymer slides were incubated in 15 ml medium inoculated with diluted (OD_{600} = 0.01) GFP-tagged bacteria from overnight cultures grown at 37 ^{o}C with 60 rpm shaking for 24 h or 72 h. As growth medium controls, the slides were also incubated without bacteria. At the desired time points, the slides were removed, and washed three times with 15 ml PBS at room temperature for 5 min. After rinsing with distilled H_2O to remove salts and air dried, the fluorescent images from the slides incubated in medium only and medium containing bacteria were acquired using a GenePix Autoloader 4200AL Scanner (Molecular Devices, US) with a 488 nm excitation laser and a blue emission filter (510-560nm). The total fluorescence intensity from polymer spots was acquired using GenePix Pro 6 software (Molecular Devices, US). A similar bacterial assay was also applied to scaled-up coupons and 4 cm sections of coated catheters. After washing with distilled H_2O, the coupons or catheters were stained with 20 µM SYTO17 dye (Invitrogen, UK) at room temperature for 30 min. After air drying, the samples were examined using a Carl Zeiss LSM 700 Laser Scanning Microscope with ZEN 2009 imaging software (Carl Zeiss, Germany). The coverage of bacteria on the surface was analysed using open source Image J 1.44 software (National Institute of Health, US). The viability of bacteria attached to polymer surfaces was assessed by live/dead staining. Briefly bacteria were stained with 10 µM SYTO 9 green-fluorescent dye for live bacteria and 60 µM propidium iodide red-fluorescent dye for cell membrane damaged (dead) bacteria. After staining at room temperature for 30 min, the samples were rinsed with distilled H_2O, air dried and observed using Laser Scanning Confocal Microscopy. To evaluate the growth

inhibitory properties of the hit polymers, polymer coated wells were UV sterilised for 15 min, and inoculated with bacteria (OD_{600} = 0.01) from overnight cultures. The OD was monitored by an Infinite 200 microplate reader (Tecan, UK) at 37°C every 30 min for 24 h to obtain the respective growth curves.

The fluorescence signal ($\mathcal{F}$) from each bacterial pathogen was determined using equation 1 where *F* is the fluorescence intensity measured per unit area by the laser scanner after incubation with bacteria and $F_{control}$ is the fluorescence intensity measured per unit area by the laser scanner measured on a control slide consisting of a replica array that was incubated in media for 72 h without bacteria. For polymers where $\mathcal{F}$ was below the limit of detection $\mathcal{F}$ was made to equal 0 (See supplementary information for further discussion).

$$\mathcal{F} = F - F_{control} \quad (1)$$

The bacterial performance (i) was determined using equation 2 where the subscript to the $\mathcal{F}$ indicates the bacterial pathogen and the $\mathcal{F}_{max}$ is the maximum fluorescence signal measured on any spot on the array for a given pathogen. Artificial urine is abbreviated to 'au'. Note that *i* reported for generation 2 arrays and scaled-up samples did not include results of UPEC in artificial urine.

$$i = \left(\frac{\mathcal{F}_{\mathrm{PA01}}}{\mathcal{F}_{\mathrm{PA01max}}} + \frac{\mathcal{F}_{8325-4}}{\mathcal{F}_{8325-4\mathrm{max}}} + \frac{\mathcal{F}_{\mathrm{UPEC}}}{\mathcal{F}_{\mathrm{UPECmax}}} + \frac{\mathcal{F}_{\mathrm{UPEC\ in\ au}}}{\mathcal{F}_{\mathrm{UPECmax\ in\ au}}} + \frac{\mathcal{F}_{\mathrm{UPEC\ on\ au\ conditioned}}}{\mathcal{F}_{\mathrm{UPECmax\ on\ au\ conditioned}}}\right) \div 5 \times 100 \quad (2)$$

Murine catheter implant model. To evaluate the *in vivo* resistance of polymer materials to bacterial attachment, the real time, non-invasive catheter foreign body implant model was used[50] (see supplementary methods). A 1 cm coated catheter segment was inserted subcutaneously into female Balb/c mice, 19-22 g (Charles River). The animals were allowed to recover with regular observation for 24 h prior to anesthesia with isoflurane and injection of $1x10^5$ *S. aureus* Xen29 (Caliper Life Sciences Inc) in 50 µl PBS into the lumen of the catheter using an 31 gauge needle and syringe. Mice were imaged for up to 5 min prior to (to assess background luminescence) and 10 min after initial bacterial inoculation and then every 24 h, using an IVIS spectrum camera (Caliper). EMLA cream was applied daily after imaging and weight and clinical condition of animals recorded.

The total photon emissions from the catheter implantation site were quantified by using the living image software package (Xenogen Corp), over a 4 day period. At day 4 the mice were humanely killed and the catheter and surrounding tissue removed, the mouse kidneys and spleen harvested, and the number of *S. aureus* Xen 29 colony forming units (cfu) present determined using standard procedures[50]. The cfu counts were normalized to the mass of tissue taken. Reported bioluminescence values had the background luminescence measured from uninoculated

inserted catheters subtracted. In each experiment, a group of 3 mice were implanted with control or coated catheters and the experiment repeated on 3 occasions with data from n=9 for each group pooled for statistical analysis.

In pilot studies, Nano-ct, computed tomographic scans were used to confirm the subcutaneous localization of the catheter and were acquired using a Nanoect/CT (Bioscan). Briefly post catheter insertion, mice were anaesthetised using isoflurane and scanned at 45 kVP, using high resolution parameters. The resulting images were reconstructed and analysed using invivoscope software.

Acknowledgments: Funding from the Wellcome Trust (grant number 085245 and support from Nicki Shepherd) and the Medical Research Council UK (for the *in vivo* work; grant number G0802525) is gratefully acknowledged . Morgan Alexander gratefully acknowledges the Royal Society for the provision of his Wolfson Research Merit Award. Assistance with ToF-SIMS measurements from David Scurr is kindly acknowledged. Assistance with the preparation of polymer for *in vivo* studies by Elizabeth Eaves, Nam Nguyen and Jianing Li is kindly acknowledged.

Author contributions: M.R.A., M.C.D, P.W., R.L. and D.G.A. conceived the high throughput strategy. Y.M., A.L.H. and J.Y. prepared the microarrays. J.Y. coated catheters with hit polymers. J.Y. and A.L.H. performed the HT-SC. C.C. performed the biological assays with support from S.A. D.I. prepared polymer for *in vivo* assays. J.L. and A.C. performed the *in vivo* assays. A.L.H., C.C., J.Y., M.R.A., M.C.D., P.W., R.B., D.G.A., and R.L. contributed to the analysis of data and the writing of the manuscript.

Fig. 1. Schematic of the approach used to identify 'hit' compositions that resist bacterial attachment. (a) The chemical structures of the monomers. (b-f) Outline of the strategy utilised for identifying hit composition. (b) Fluorescence scanner image of the first generation microarray after incubation with *P. aeruginosa* for 72 h. 3 replicate arrays were present on each glass slides. Scale bar is 10 mm. (c) Intensity map of the bacterial data from the first generation array. (d) The feedback loop used to select monomer compositions for a second generation array. The biological performance of each monomer, the identification of hit compositions that display synergistic effects and the results from the PLS regression of ToF-SIMS spectra and bacterial data were used to inform the composition of the second generation array. (e) Schematic representation of the hit composition scaled up. (f) An SEM image of the cross-section of a silicone catheter coated with a 'hit' polymer (thickness = 20-25 µm). The scale bar is 100 µm. (g) Confocal images of SYTO17 stained biofilm for the 3 pathogens studied (*P. aeruginosa* (PA), *S. aureus* (SA), UPEC) from coated and uncoated silicone catheters. Each image is 160 x 160 µm. (h) Nano-ct tomographic scan of a coated catheter implanted subcutaneously into a murine model. To highlight, the catheter has been false coloured green. (i) A schematic representation of a catheter coated with the hit composition.

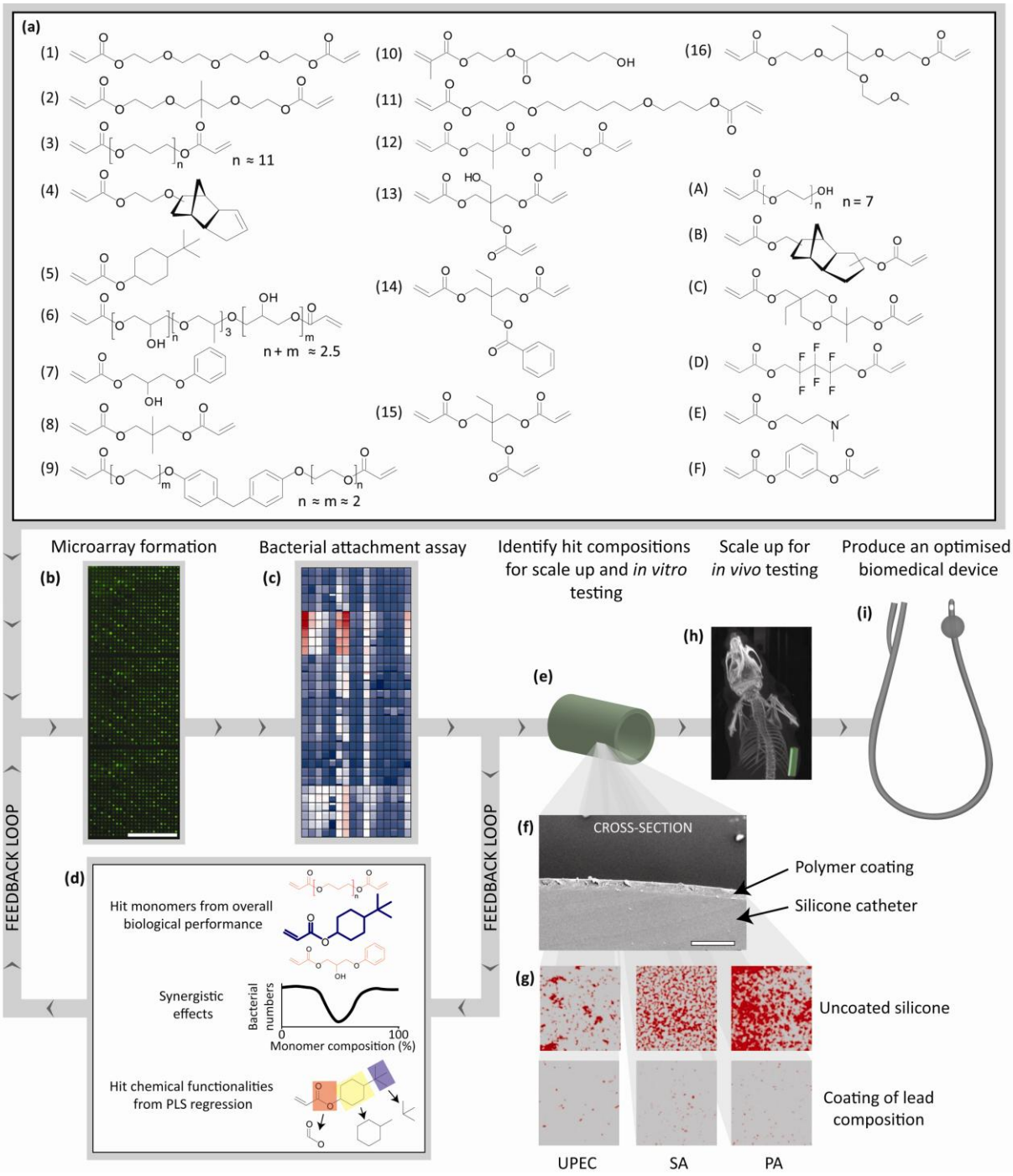

Fig. 2. (a) Schematic of the bacterial attachment assay. Bacterial strains were transformed with GFP and grown in LB broth overnight. The polymer microarray was inoculated with bacteria in RPMI1640 medium and after incubation the fluorescence on each spot quantified using a fluorescence scanner. (b-f) Intensity map of $\mathcal{I}$ measured for each bacterial strain on the first generation array after 72 h incubation; (b) *P. aeruginosa*, (c) *S. aureus,* (d) UPEC, (e) UPEC grown in artificial urine, and (f) UPEC grown on an artificial urine conditioned slide. (g) Intensity map of the i obtained for each material in the array. The major monomers are listed on the y-axis whilst the composition of the minor monomers is shown in the x-axis. The large shaded area within each outlined area indicates the mean value and the mean ± one standard deviation unit is presented in the narrow columns to the right (plus) and left (minus) of the mean, n=3. (h) The average i for all materials containing a specific monomer, ranked from lowest to highest. The major and minor monomers were considered separately. The colour next to each monomer is indicative of that monomer's mean i and is coloured by the same intensity scale of (g).

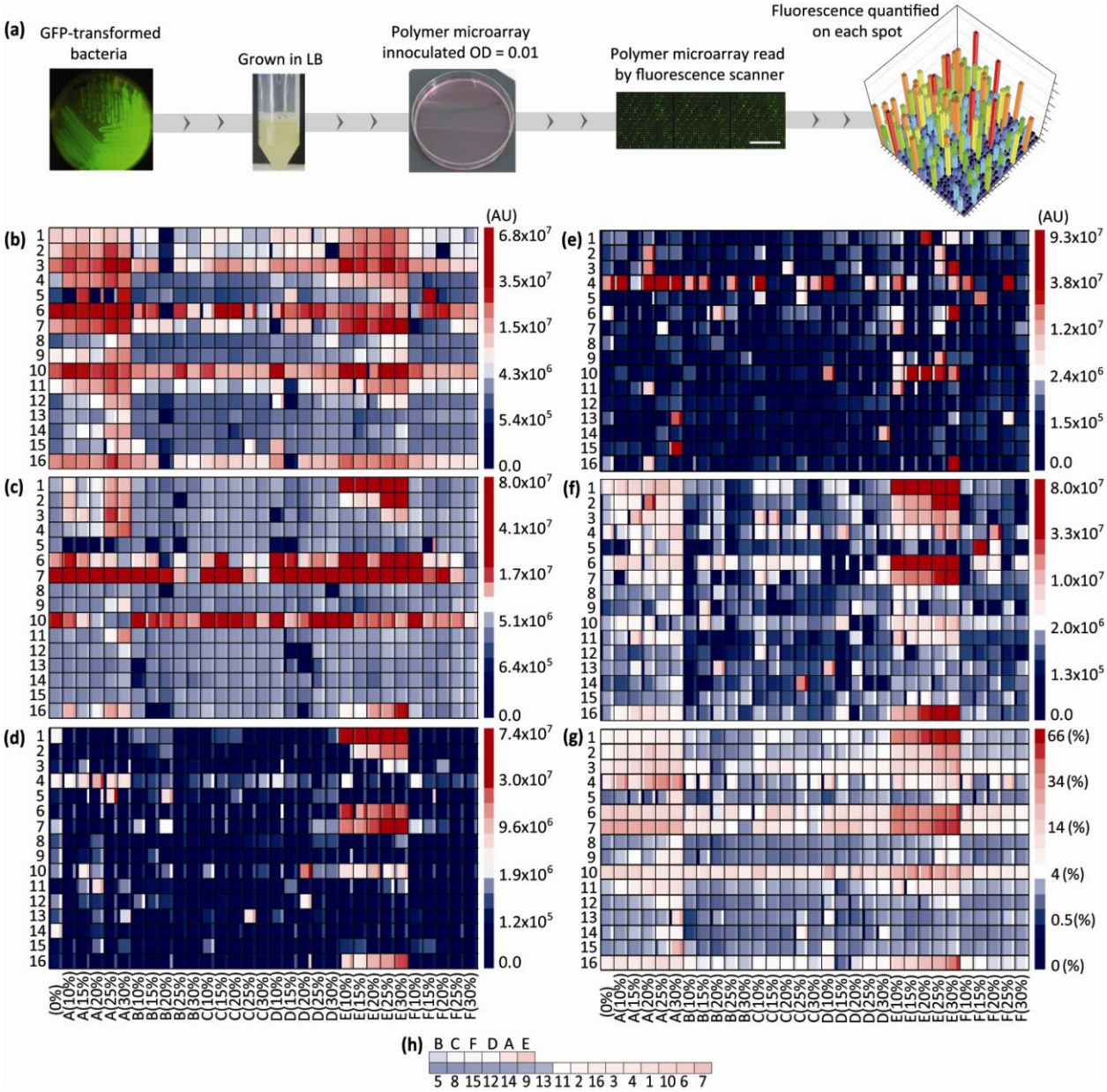

Fig. 3. (a) Schematic depiction of the PLS regression model used to predict the biological performance of materials by correlating $\mathcal{F}$ with the ToF-SIMS spectra. (b-d) The predicted bacterial attachment determined from the PLS regression model for (b) *P. aeruginosa* (PA) (R^2=0.68), (c) *S. aureus* (SA) (R^2=0.76), and (d) UPEC (R^2=0.28). The y=x line is drawn as a guide. Polymers are grouped according to the major monomer 1 (×), 2 (○), 3 (×), 4 (○), 5 (×), 6 (○), 7 (×), 8 (○), 9 (×), 10 (○), 11 (×), 12 (○), 13 (×), 14 (○), 15 (×), 16 (○). (e) The key ions identified to be important by ToF-SIMS PLS regression analysis for the surface attachment of both *P. aeruginosa* (PA) and *S. aureus* (SA). The regression coefficient (RC) for each ion is also shown from the regression analysis with each bacterium separately. The RCs have been shaded according to their value (red = positive, blue = negative).

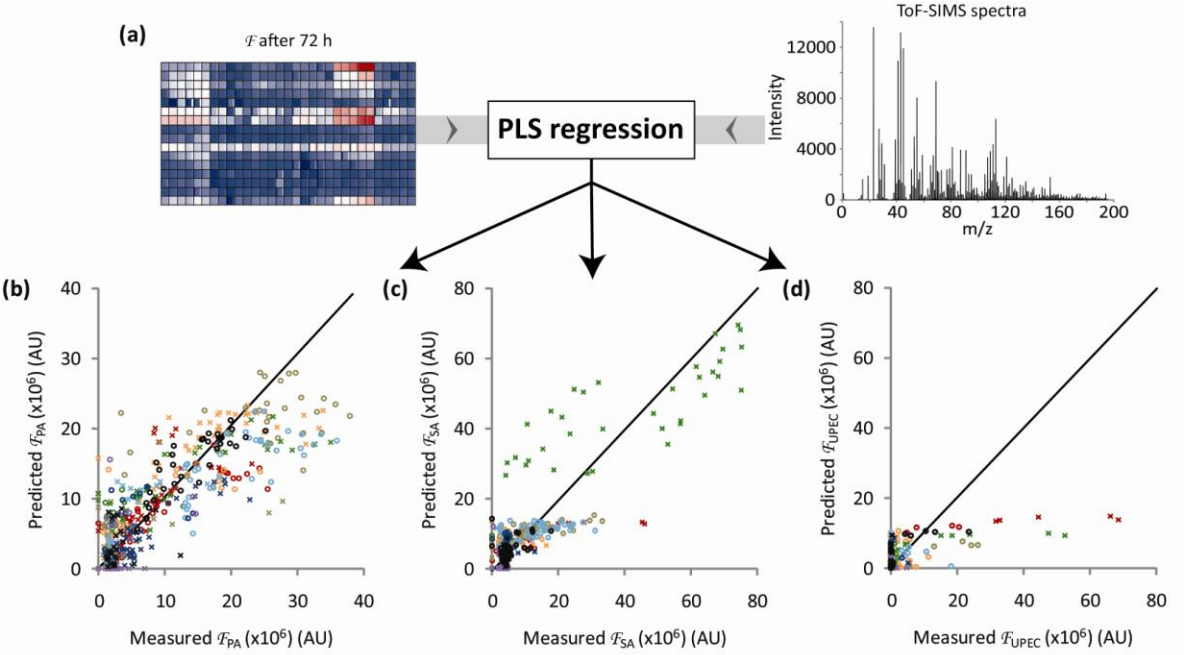

(e)

Ion	Positive RC_{PA} (x10^7)	Positive RC_{SA} (x10^7)	Ion	Negative RC_{PA} (x10^7)	Negative RC_{SA} (x10^7)
$C_2H_5O^+$	8.1	-0.2	C_2H^-	-7.8	-5
$C_3H_7O^+$	7.4	1.4	C_4H^-	-3.3	-1.6
$C_6H_5O^-$	4.4	26.9	$C_3H_3^+$	-2.5	-0.8
$C_6H_{11}O_3^-$	4.4	1.3	$C_2H_3^+$	-2.3	-1.6
$C_5H_9^+$	3.6	1	$C_8H_{15}^+$	-2.2	-1.1
$C_2H_3O^+$	3.1	0.1	$C_4H_7^+$	-2.2	-2.4
$C_3H_3O^+$	0.6	2.7	$C_3H_7^+$	-2.1	-2
$C_6H_7O^+$	0.4	1.8	$C_4H_5^+$	-1.7	-1.1
$C_6H_6O^+$	0.2	2.2	C_6H^-	-1.7	-0.8
$C_2H_3O_2^-$	0.1	2.2	CHO_2^-	-1.5	-2.1
$C_4H_5O_2^-$	0.1	2	$C_4H_7O^-$	-1.5	-0.4
$C_3H_3O_2^-$	0	4.5	$C_2H_5^+$	-1.4	-1
$C_7H_7O^+$	0	2.6	$C_4H_3^+$	-1.1	-0.4
$C_6H_5^+$	-0.5	5.4	$C_3H_5^+$	-0.5	-1.5
			$C_7H_5O_2^-$	0	-1.4
			$C_7H_5O^+$	1.4	-1.9

Fig. 4. *i* determined for all materials represented in the second generation array. 5 monomers from the first generation array were mixed pairwise at 14 different ratios. The % content of the major monomer is indicated along the x-axis: (a) 15, (b) 8, (c) 4, (d) B and (e) 5 (Fig. 1a). The co-monomer is indicated in the y-axis. (f) The *i* determined for high bacterial attachment polymers included in the second generation array from the first generation array. The colour bar is non-linear to highlight the low *i* measured for this array. The mean of each value is shown as the large shaded area within each outlined rectangle and the mean ± one standard deviation unit is presented in the narrow columns to the right (plus) and left (minus) of the mean, n=4.

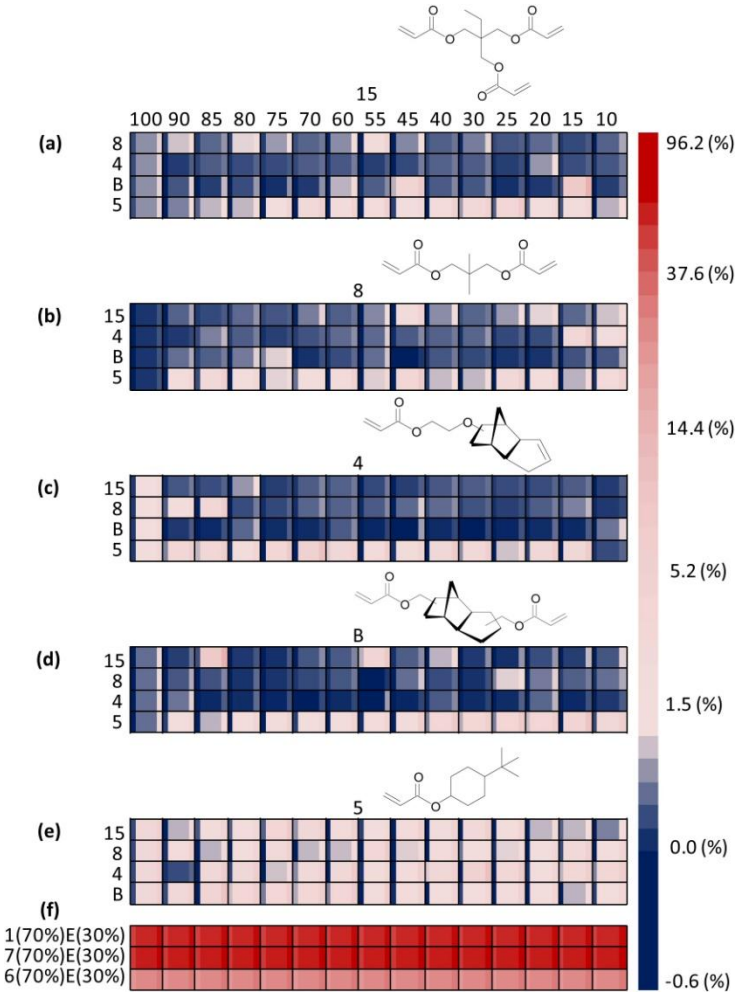

Fig. 5. Bacterial coverage on catheters coated with hit polymers after 72 hours culture. (a) Confocal microscopy images of *P. aeruginosa*, *S. aureus* and UPEC stained with SYTO17 growing on coated catheters, unmodified silicone and silicone treated with media without bacteria as a control. Each image is 160 x 160 µm. (b) quantification of bacterial surface coverage for *P. aeruginosa* (■), *S. aureus* (■), UPEC (■) and *i* (■) from confocal images of each sample. Coverage was normalised to the coverage on silicone. The error bars represent ± one standard deviation unit, n=5. The composition of the positive control was specific to the bacterial strain used: *P. aeruginosa* = 6(100%), *S. aureus* = 7(100%), UPEC = 1(70%)E(30%). The fluorescence signal observed on the media-only controls is due to auto-fluorescence of the substrate and translates to a small erroneous (<0.5%) estimate of bacterial coverage.

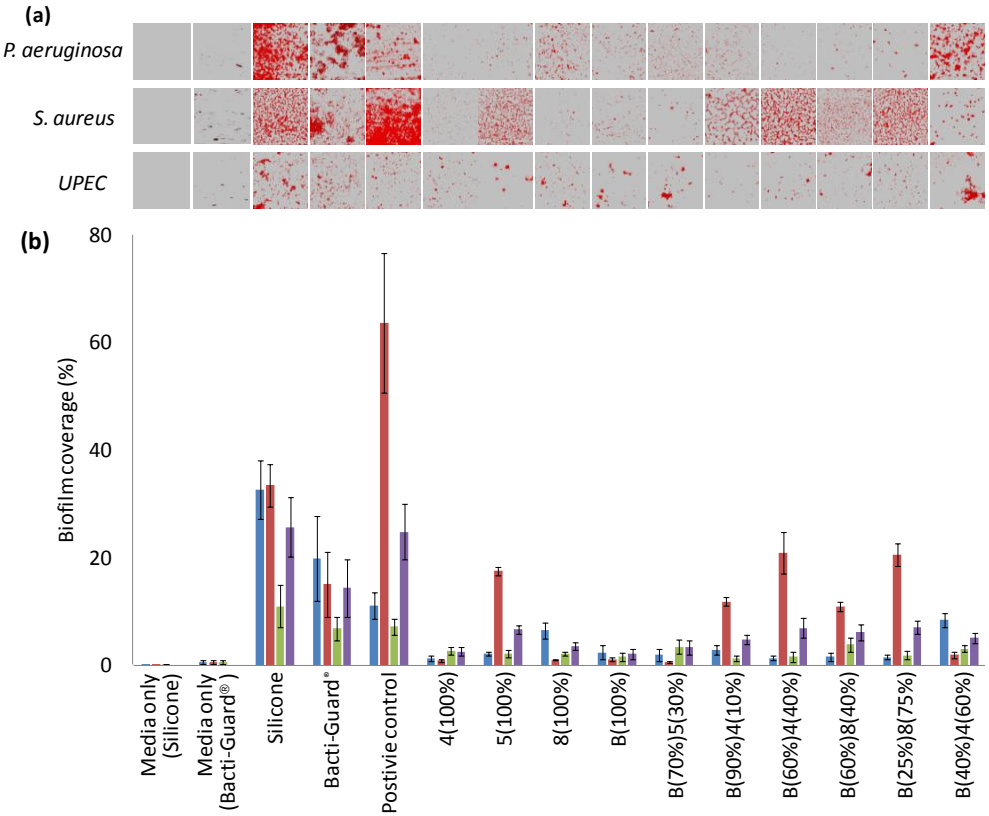

Fig. 6. *In vivo* performance of 'hit' polymer. Catheters dip-coated with hit polymer 4-co-DEGMA were implanted subcutaneously within mice and inoculated with *S. aureus Xen29*. (a) The bioluminescence at the infection site was measured on the day of inoculation (day 0) and for the next 4 days. Measurements were taken for both uncoated (■) and coated (■) silicone catheters. The error bars represent ± one standard deviation unit, n=9 (3 groups of 3 mice assessed separately). The difference in bioluminescence between coated and uncoated samples from days 1-4 was confirmed to 99.5% confidence (*t*-test). Bioluminescence was normalised to the output at day 0 and all measurements have had the background luminescence subtracted, measured prior to catheter innoculation. (b-c) Luminescence images with overlaid bright field images of mice implanted with both uncoated (left) and coated (right) catheter segments on day 0 (b) and day 4 (c). (d) At day 4 the mice were sacrificed, the insertion site plus the kidneys and spleen harvested, and the number of bacteria on the tissue determined. Measurements were taken for both uncoated (■) and coated (■) silicone catheters. The error bars represent ± one standard deviation unit, n=3 (taken from 1 group of 3). The difference in cfu counts between coated and uncoated samples was confirmed to 99% confidence for the catheter and surrounding tissue, to 90% confidence for the kidneys and to 75% confidence for the spleen (*t*-test).

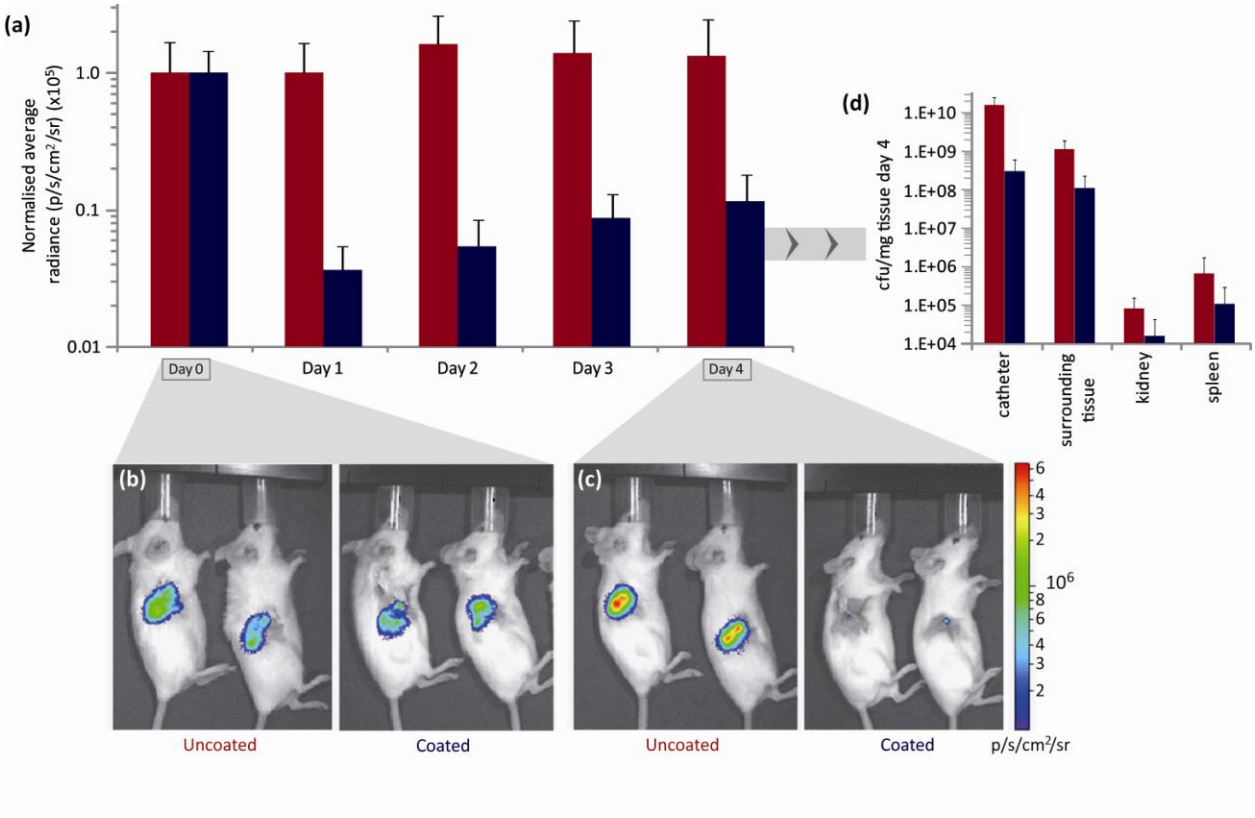

References

1 Davies, D. Understanding biofilm resistance to antibacterial agents. *Nat. Rev. Drug Discovery* **2**, 114-122, (2003).

2 Costerton, J. W., Stewart, P. S. & Greenberg, E. P. Bacterial biofilms: A common cause of persistent infections. *Science* **284**, 1318-1322, (1999).

3 Smith, A. W. Biofilms and antibiotic therapy: Is there a role for combating bacterial resistance by the use of novel drug delivery systems? *Adv. Drug Deliver. Rev.* **57**, 1539-1550, (2005).

4 Danese, P. N. Antibiofilm approaches: Prevention of catheter colonization. *Chem. Biol.* **9**, 873-880, (2002).

5 Krol, J. E. *et al.* Increased Transfer of a Multidrug Resistance Plasmid in Escherichia coli Biofilms at the Air-Liquid Interface. *Appl. Environ. Microb.* **77**, 5079-5088, (2011).

6 Darouiche, R. O. *et al.* A comparison of two antimicrobial-impregnated central venous catheters. *New Engl. J. Med.* **340**, 1-8, (1999).

7 Raad, I. *et al.* Central venous catheters coated with minocycline and rifampin for the prevention of catheter-related colonization and bloodstream infections - A randomized, double-blind trial. *Ann. Intern. Med.* **127**, 267-&, (1997).

8 Yorganci, K., Krepel, C., Weigelt, J. A. & Edmiston, C. E. Activity of antibacterial impregnated central venous catheters against Klebsiella pneumoniae. *Intens. Care Med.* **28**, 438-442, (2002).

9 Jaeger, K. *et al.* Efficacy of a benzalkonium chloride-impregnated central venous catheter to prevent catheter-associated infection in cancer patients. *Chemotherapy* **47**, 50-55, (2001).

10 Greenfeld, J. I. *et al.* Decreased bacterial adherence and biofilm formation on chlorhexidine and silver sulfadiazine-impregnated cnetral venous catheters implanted in swine. *Crit. Care Med.* **23**, 894-900, (1995).

11 Guay, D. R. An update on the role of nitrofurans in the management of urinary tract infections. *Drugs* **61**, 353-364, (2001).

12 Caillier, L. *et al.* Synthesis and antimicrobial properties of polymerizable quaternary ammoniums. *Eur. J. Med. Chem.* **44**, 3201-3208, (2009).

13 Darouiche, R. O., Mansouri, M. D., Gawande, P. V. & Madhyastha, S. Efficacy of combination of chlorhexidine and protamine sulphate against device-associated pathogens. *J. Antimicrob. Chemoth.* **61**, 651-657, (2008).

14 Li, P. *et al.* A polycationic antimicrobial and biocompatible hydrogel with microbe membrane suctioning ability. *Nat. Mater.* **10**, 149-156, (2011).

15 Costa, F., Carvalho, I. F., Montelaro, R. C., Gomes, P. & Martins, M. C. L. Covalent immobilization of antimicrobial peptides (AMPs) onto biomaterial surfaces. *Acta Biomater.* **7**, 1431-1440, (2011).

16 Monds, R. D. & O'Toole, G. A. The developmental model of microbial biofilms: ten years of a paradigm up for review. *Trends Microbiol.* **17**, 73-87, (2009).

17 Holmes, P. F. *et al.* Surface-modified nanoparticles as a new, versatile, and mechanically robust nonadhesive coating: Suppression of protein adsorption and bacterial adhesion. *J. Biomed. Mater. Res. A* **91A**, 824-833, (2009).

18 Cheng, G. *et al.* Zwitterionic carboxybetaine polymer surfaces and their resistance to long-term biofilm formation. *Biomaterials* **30**, 5234-5240, (2009).

19 Cheng, G., Zhang, Z., Chen, S. F., Bryers, J. D. & Jiang, S. Y. Inhibition of bacterial adhesion and biofilm formation on zwitterionic surfaces. *Biomaterials* **28**, 4192-4199, (2007).

20 Hook, A. L. *et al.* High throughput methods applied in biomaterial development and discovery. *Biomaterials* **31**, 187-198, (2010).

21 Pernagallo, S., Wu, M., Gallagher, M. P. & Bradley, M. Colonising new frontiers-microarrays reveal biofilm modulating polymers. *J. Mater. Chem.* **21**, 96-101, (2011).

22 Anderson, D. G., Levenberg, S. & Langer, R. Nanoliter-scale synthesis of arrayed biomaterials and application to human embryonic stem cells. *Nat. Biotechnol.* **22**, 863-866, (2004).

23 Mei, Y. *et al.* Mapping the Interactions among Biomaterials, Adsorbed Proteins, and Human Embryonic Stem Cells. *Adv. Mater.* **21**, 2781-2786, (2009).

24 Mei, Y. *et al.* Combinatorial development of biomaterials for clonal growth of human pluripotent stem cells. *Nat. Mater.* **9**, 768-778, (2010).

25 Yang, J. *et al.* Polymer surface functionalities that control human embryoid body cell adhesion revealed by high throughput surface characterization of combinatorial material microarrays. *Biomaterials* **31**, 8827-8838, (2010).

26 Berger, H., Hacker, J., Juarez, A., Hughes, C. & Goebel, W. Cloning of the chromosomal determinants encoding hemolysin production and mannose-resistant hemagglutination in Escherichia-coli. *J. Bacteriol.***152**, 1241-1247, (1982).

27 Hidron, A. I. *et al.* Antimicrobial-Resistant Pathogens Associated With Healthcare-Associated Infections: Annual Summary of Data Reported to the National Healthcare Safety Network at the Centers for Disease Control and Prevention, 2006-2007. *Infect. Cont. Hosp. Ep.* **29**, 996-1011, (2008).

28 Katsikogianni, M. & Missirlis, Y. F. Concise review of mechanisms of bacterial adhesion to biomaterials and of techniques used in estimating bacteria-material interactions. *Eur. Cells Mater.* **8**, 37-57, (2004).

29 O'Toole, G., Kaplan, H. B. & Kolter, R. Biofilm formation as microbial development. *Annu. Rev. Microbiol.* **54**, 49-79, (2000).

30 Flemming, H. C. & Wingender, J. The biofilm matrix. *Nat. Rev. Microbiol.* **8**, 623-633, (2010).

31 Urquhart, A. J. *et al.* High throughput surface characterisation of a combinatorial material library. *Adv. Mater.* **19**, 2486-2491, (2007).

32 Davies, M. C. *et al.* High throughput surface characterization: A review of a new tool for screening prospective biomedical material arrays. *J. Drug Target.* **18**, 741-751, (2010).

33 Hook, A. L. *et al.* Polymers with hydro-responsive topography identified using high throughput AFM of an acrylate microarray. *Soft Matter* **7**, 7194-7197, (2011).

34 Taylor, M., Urquhart, A. J., Zelzer, M., Davies, M. C. & Alexander, M. R. Picoliter water contact angle measurement on polymers. *Langmuir* **23**, 6875-6878, (2007).

35 Taylor, M. *et al.* Partial least squares regression as a powerful tool for investigating large combinatorial polymer libraries. *Surf. Interface Anal.* **41**, 127-135, (2009).

36 Schumm, K. & Lam, T. B. Types of urethral catheters for management of short-term voiding problems in hospitalised adults. *Cochrane DB. Syst. Rev.* **16**, CD004013, (2008).

37 Dalton, H. M. & March, P. E. in *Handbook of bacterial adhesion: principles, methods, and applications* eds Y. H. An & R. J. Friedman (Humana Press, 2000).

38 Ong, Y. L., Razatos, A., Georgiou, G. & Sharma, M. M. Adhesion forces between E-coli bacteria and biomaterial surfaces. *Langmuir* **15**, 2719-2725, (1999).

39 Conrad, J. C. C. J. C. *et al.* Flagella and Pili-Mediated Near-Surface Single-Cell Motility Mechanisms in P. aeruginosa. *Biophys. J.* **100**, 1608-1616, (2011).

40 Williams, P., Winzer, K., Chan, W. C. & Camara, M. Look who's talking: communication and quorum sensing in the bacterial world. *Philos. T. R. Soc. B* **362**, 1119-1134, (2007).

41 Ferrieres, L. & Clarke, D. J. The RcsC sensor kinase is required for normal biofilm formation in Escherichia coli K-12 and controls the expression of a regulon in response to growth on a solid surface. *Mol. Microbiol.* **50**, 1665-1682, (2003).

42 Gilbert, K. B., Kim, T. H., Gupta, R., Greenberg, E. P. & Schuster, M. Global position analysis of the Pseudomonas aeruginosa quorum-sensing transcription factor LasR. *Mol. Microbiol.* **73**, 1072-1085, (2009).

43 Harder, P., Grunze, M., Dahint, R., Whitesides, G. M. & Laibinis, P. E. Molecular conformation in oligo(ethylene glycol)-terminated self-assembled monolayers on gold and silver surfaces determines their ability to resist protein adsorption. *J. Phys. Chem. B* **102**, 426-436, (1998).

44 Urquhart, A. J. *et al.* TOF-SIMS analysis of a 576 micropatterned copolymer array to reveal surface moieties that control wettability. *Anal. Chem.* **80**, 135-142, (2008).

45 Messina, M. *Gene Regulation in Pseudomonas aeruginosa: from environmental signals to responses via global post-transcriptional control and intracellular messaging* PhD thesis, University of Nottingham, (2010).

46 Qazi, S. N. A., Rees, C. E. D., Mellits, K. H. & Hill, P. J. Development of gfp vectors for expression in Listeria monocytogenes and other low G+C gram positive bacteria. *Microbial Ecol.* **41**, 301-309, (2001).

47 Brooks, T. & Keevil, C. W. A simple artificial urine for the growth of urinary pathogens. *Lett. Appl. Microbiol.* **24**, 203-206, (1997).

48 Diggle, S. P. *et al.* The galactophilic lectin, LecA, contributes to biofilm development in Pseudomonas aeruginosa. *Environ. Microbiol.* **8**, 1095-1104, (2006).

49 Johansson, E. M. V. *et al.* Inhibition and Dispersion of Pseudomonas aeruginosa Biofilms by Glycopeptide Dendrimers Targeting the Fucose-Specific Lectin LecB. *Chem. Biol.* **15**, 1249-1257, (2008).

50 Kuklin, N. A. *et al.* Real-time monitoring of bacterial infection in vivo: Development of bioluminescent staphylococcal foreign-body and deep-thigh-wound mouse infection models. *Antimicrob. Agents Ch.* **47**, 2740-2748, (2003).